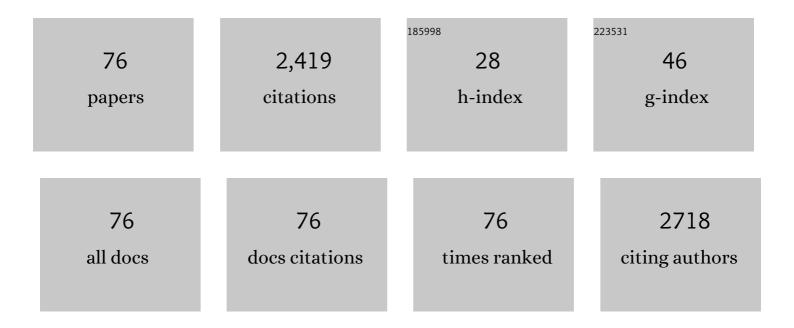
## List of Publications by Year in descending order

Source: https://exaly.com/author-pdf/575763/publications.pdf Version: 2024-02-01



l et l tri

#	Article	IF	CITATIONS
1	Synergistic effect of surface textures and DLC coatings for enhancing friction and wear performances of Si3N4/TiC ceramic. Ceramics International, 2022, 48, 514-524.	2.3	44
2	MoS <sub>2</sub> /MXene Aerogel with Conformal Heterogeneous Interfaces Tailored by Atomic Layer Deposition for Tunable Microwave Absorption. Advanced Science, 2022, 9, e2101988.	5.6	76
3	Advances in Laser Drilling of Structural Ceramics. Nanomaterials, 2022, 12, 230.	1.9	48
4	Fabrication and properties of micro-additive manufactured Ni-based composite coatings by short-pulsed laser. Optics and Laser Technology, 2022, 150, 107973.	2.2	4
5	Atomic Layer Deposition-Made MoS <sub>2</sub> –ReS <sub>2</sub> Nanotubes with Cylindrical Wall Heterojunctions for Ultrasensitive MiRNA-155 Detection. ACS Applied Materials & Interfaces, 2022, 14, 10081-10091.	4.0	7
6	Pt Atom on the Wall of Atomic Layer Deposition (ALD)â€Made MoS <sub>2</sub> Nanotubes for Efficient Hydrogen Evolution. Small, 2022, 18, e2105129.	5.2	29
7	Ultrasensitive Surfaceâ€Enhanced Raman Scattering (SERS) Detection For miRNAâ€182 Based on CdS/MoS <sub>2</sub> @AuNPs Fabricated by Atomic Layer Deposition (ALD). Advanced Materials Interfaces, 2022, 9, .	1.9	2
8	A novel 1D/2D interpenetrating network architecture of MXene/cellulose composite microfiber and graphene for broadband microwave absorption. Chemical Engineering Journal, 2022, 439, 135734.	6.6	29
9	Ultralow-Voltage-Drivable Artificial Muscles Based on a 3D Structure MXene-PEDOT:PSS/AgNWs Electrode. ACS Applied Materials & Interfaces, 2022, 14, 18150-18158.	4.0	24
10	Nanometer-Thick MoS <sub>2</sub> Films Made by High-Temperature Atomic Layer Deposition as Coatings for Friction Reduction. ACS Applied Nano Materials, 2022, 5, 5652-5659.	2.4	3
11	Numerical analyses of rectangular micro-textures in hydrodynamic lubrication regime for sliding contacts. Meccanica, 2021, 56, 365-382.	1.2	13
12	Nanocrystalline NiSe <sub>2</sub> /MoS <sub>2</sub> heterostructures for electrochemical hydrogen evolution reaction. Nanotechnology, 2021, 32, 175602.	1.3	11
13	Ultrasensitive photoelectrochemical detection of cancer-related miRNA-141 by carrier recombination inhibition in hierarchical Ti3C2@ReS2. Sensors and Actuators B: Chemical, 2021, 331, 129470.	4.0	20
14	Tribological characteristics and advanced processing methods of textured surfaces: a review. International Journal of Advanced Manufacturing Technology, 2021, 114, 1241-1277.	1.5	58
15	Formation of bionic surface textures composed by micro-channels using nanosecond laser on Si3N4-based ceramics. Ceramics International, 2021, 47, 12768-12779.	2.3	41
16	MoSe <sub>2</sub> /CdSe Heterojunction Destruction by Cation Exchange for Photoelectrochemical Immunoassays with a Controlled-Release Strategy. Analytical Chemistry, 2021, 93, 10712-10718.	3.2	22
17	Ultrathin molybdenum disulfide (MoS2) film obtained in atomic layer deposition: A mini-review. Science China Technological Sciences, 2021, 64, 2347-2359.	2.0	8
18	MoS2 with Controlled Thickness for Electrocatalytic Hydrogen Evolution. Nanoscale Research Letters, 2021, 16, 137.	3.1	17

#	Article	IF	CITATIONS
19	Nanotribological properties of 2-D MoS2 on different substrates made by atomic layer deposition (ALD). Applied Surface Science, 2020, 502, 144402.	3.1	15
20	Direct fabrication of two-dimensional ReS <sub>2</sub> on SiO <sub>2</sub> /Si substrate by a wide-temperature-range atomic layer deposition. Nanotechnology, 2020, 31, 055602.	1.3	6
21	CuS@defect-rich MoS2 core-shell structure for enhanced hydrogen evolution. Journal of Colloid and Interface Science, 2020, 564, 77-87.	5.0	44
22	Ultrasensitive SERS Detection of Cancerâ€Related miRNAâ€182 by MXene/MoS <sub>2</sub> @AuNPs with Controllable Morphology and Optimized Selfâ€Internal Standards. Advanced Optical Materials, 2020, 8, 2001214.	3.6	51
23	Ultrathin Quasibinary Heterojunctioned ReS <sub>2</sub> /MoS <sub>2</sub> Film with Controlled Adhesion from a Bimetallic Co-Feeding Atomic Layer Deposition. ACS Applied Materials & Interfaces, 2020, 12, 43311-43319.	4.0	10
24	Hierarchical Carbon Fiber@MXene@MoS <sub>2</sub> Coreâ€sheath Synergistic Microstructure for Tunable and Efficient Microwave Absorption. Advanced Functional Materials, 2020, 30, 2002595.	7.8	311
25	Plasma-assisted friction control of 2D MoS <sub>2</sub> made by atomic layer deposition. Nanotechnology, 2020, 31, 395711.	1.3	7
26	MoS <sub>2</sub> -ReS <sub>2</sub> Heterojunctions from a Bimetallic Co-chamber Feeding Atomic Layer Deposition for Ultrasensitive MiRNA-21 Detection. ACS Applied Materials & Interfaces, 2020, 12, 29074-29084.	4.0	5
27	Numerical investigation of the performance of micro-textured cutting tools in cutting of Ti-6Al-4V alloys. International Journal of Advanced Manufacturing Technology, 2020, 108, 463-474.	1.5	23
28	A Novel Biosensor Based on Molybdenum Disulfide (MoS <sub>2</sub> ) Modified Porous Anodic Aluminum Oxide Nanochannels for Ultrasensitive microRNAâ€155 Detection. Small, 2020, 16, e2001223.	5.2	52
29	Synergistic lubrication of a porous MoS <sub>2</sub> -POSS nanohybrid. RSC Advances, 2020, 10, 20579-20587.	1.7	6
30	Assessment machining of micro-channel textures on PCD by laser-induced plasma and ultra-short pulsed laser ablation. Optics and Laser Technology, 2020, 125, 106057.	2.2	14
31	LIPSS combined with ALD MoS2 nano-coatings for enhancing surface friction and hydrophobic performances. Surface and Coatings Technology, 2020, 385, 125396.	2.2	31
32	A simple strategy for the detection of Cu( <scp>ii</scp> ), Cd( <scp>ii</scp> ) and Pb( <scp>ii</scp> ) in water by a voltammetric sensor on a TC4A modified electrode. New Journal of Chemistry, 2019, 43, 1544-1550.	1.4	20
33	Friction-Induced Enhancements for Photocatalytic Degradation of MoS <sub>2</sub> @Ti <sub>3</sub> C <sub>2</sub> Nanohybrid. Industrial & Engineering Chemistry Research, 2019, 58, 18141-18148.	1.8	34
34	Ultrasensitive detection of miRNA-155 based on controlled fabrication of AuNPs@MoS2 nanostructures by atomic layer deposition. Biosensors and Bioelectronics, 2019, 144, 111660.	5.3	47
35	Trickle Flow Aided Atomic Layer Deposition (ALD) Strategy for Ultrathin Molybdenum Disulfide (MoS <sub>2</sub> ) Synthesis. ACS Applied Materials & Interfaces, 2019, 11, 36270-36277.	4.0	26
36	A novel label-free strategy for the ultrasensitive miRNA-182 detection based on MoS2/Ti3C2 nanohybrids. Biosensors and Bioelectronics, 2019, 137, 45-51.	5.3	79

#	Article	IF	CITATIONS
37	Recent progress in atomic layer deposition of molybdenum disulfide: a mini review. Science China Materials, 2019, 62, 913-924.	3.5	24
38	Nanotribological Properties of ALD-Made Ultrathin MoS <sub>2</sub> Influenced by Film Thickness and Scanning Velocity. Langmuir, 2019, 35, 3651-3657.	1.6	16
39	Drastically Reduced Ion Mobility in a Nanopore Due to Enhanced Pairing and Collisions between Dehydrated Ions. Journal of the American Chemical Society, 2019, 141, 4264-4272.	6.6	46
40	Modulated electrochemical oxygen evolution catalyzed by MoS <sub>2</sub> nanoflakes from atomic layer deposition. Nanotechnology, 2019, 30, 095402.	1.3	22
41	Nanopore-Based Strategy for Sequential Separation of Heavy-Metal Ions in Water. Environmental Science & Technology, 2018, 52, 5884-5891.	4.6	30
42	Dependence of the friction strengthening of graphene on velocity. Nanoscale, 2018, 10, 1855-1864.	2.8	31
43	A Green Design for Lubrication: Multifunctional System Containing Fe <sub>3</sub> O <sub>4</sub> @MoS <sub>2</sub> Nanohybrid. ACS Sustainable Chemistry and Engineering, 2018, 6, 7372-7379.	3.2	27
44	Enhanced Lubrication and Photocatalytic Degradation of Liquid Paraffin by Hollow MoS <sub>2</sub> Microspheres. ACS Omega, 2018, 3, 3120-3128.	1.6	14
45	Pressure-assisted synthesis of a polyaniline–graphite oxide (PANI–GO) hybrid and its friction reducing behavior in liquid paraffin (LP). New Journal of Chemistry, 2018, 42, 936-942.	1.4	9
46	Fabrication and characterization of micro-channels on Al2O3/TiC ceramic produced by nanosecond laser. Ceramics International, 2018, 44, 23035-23044.	2.3	56
47	Micro-channels machining on polycrystalline diamond by nanosecond laser. Optics and Laser Technology, 2018, 108, 333-345.	2.2	38
48	MoS2 solid-lubricating film fabricated by atomic layer deposition on Si substrate. AIP Advances, 2018, 8, .	0.6	16
49	Controllable Nanotribological Properties of Graphene Nanosheets. Scientific Reports, 2017, 7, 41891.	1.6	27
50	Preparation and characterization of molybdenum disulfide films obtained by one-step atomic layer deposition method. Thin Solid Films, 2017, 624, 101-105.	0.8	28
51	MoS 2 hollow microspheres used as a green lubricating additive for liquid paraffin. Tribology International, 2017, 114, 315-321.	3.0	38
52	Layer-controlled precise fabrication of ultrathin MoS <sub>2</sub> films by atomic layer deposition. Nanotechnology, 2017, 28, 195605.	1.3	39
53	Nanotribological characterization of graphene on soft elastic substrate. Carbon, 2017, 124, 541-546.	5.4	38
54	Investigation on pyrolysis of intumescent flame-retardant polypropylene (PP) composites based on synchrotron vacuum ultraviolet photoionization combined with molecular-beam mass spectrometry. Journal of Thermal Analysis and Calorimetry, 2017, 130, 1003-1009.	2.0	13

#	Article	IF	CITATIONS
55	Enhanced lubrication and photocatalytic degradation of liquid paraffin by coral-like MoS <sub>2</sub> . New Journal of Chemistry, 2017, 41, 7674-7680.	1.4	12
56	Self-assembly of zinc hydroxystannate on amorphous hydrous TiO2 solid sphere for enhancing fire safety of epoxy resin. Journal of Hazardous Materials, 2017, 340, 263-271.	6.5	37
57	Size-dependent piezoelectricity of molybdenum disulfide (MoS2) films obtained by atomic layer deposition (ALD). Applied Physics Letters, 2017, 111, .	1.5	19
58	Fabrication of coral-like MoS2 and its application in improving the tribological performance of liquid paraffin. Tribology International, 2016, 104, 303-308.	3.0	41
59	Polystyrene nanocomposites with improved combustion properties by using TMA-POSS and organic clay. Journal of Thermal Analysis and Calorimetry, 2016, 124, 743-749.	2.0	13
60	Pressure-assisted synthesis and morphology control of polyaniline. International Journal of Polymeric Materials and Polymeric Biomaterials, 2016, 65, 310-314.	1.8	1
61	xmlns:mml="http://www.w3.org/1998/Math/MathML"> < mml:mrow> < mml:mi mathvariant="normal">S  < mml:msub> < mml:mi mathvariant="normal">i < /mml:mi> < mml:mn>3 < /mml:mn> < /mml:msub> < mml:msub> < mml:mi mathvariant="normal">N < /mml:mi> < mml:mn>4 < /mml:msub> < /mml:msub> < /mml:mrow> < /mml:math> nanopores.	0.8	16
62	Physical Review E. 2015, 92, 022719. Experimental and theoretical investigations on temperature modulated translocation of IgG molecules through nanopore arrays. Analyst, The, 2015, 140, 4895-4902.	1.7	3
63	Preparation and tribological properties of organically modified graphite oxide in liquid paraffin at ultra-low concentrations. RSC Advances, 2015, 5, 90525-90530.	1.7	22
64	Thermal oxidative degradation kinetics of novel intumescent flame-retardant polypropylene composites. Journal of Thermal Analysis and Calorimetry, 2015, 120, 1183-1191.	2.0	33
65	Thermal decomposition of polypropylene by tunable synchrotron vacuum ultraviolet photoionization mass spectrometry. Journal of Thermal Analysis and Calorimetry, 2014, 118, 295-298.	2.0	4
66	Plasma Modified MoS <sub>2</sub> Nanoflakes for Surface Enhanced Raman Scattering. Small, 2014, 10, 1090-1095.	5.2	129
67	Voltage-driven translocation behaviors of IgG molecule through nanopore arrays. Nanoscale Research Letters, 2013, 8, 229.	3.1	6
68	Detecting a single molecule using a micropore-nanopore hybrid chip. Nanoscale Research Letters, 2013, 8, 498.	3.1	4
69	Highly Sensitive and Selective DNA-Based Detection of Mercury(II) with α-Hemolysin Nanopore. Journal of the American Chemical Society, 2011, 133, 18312-18317.	6.6	203
70	Novel PS Composites by Using Artificial Lamellar Hybrid from Octa(Î <sup>3</sup> -chloroaminopropyl) POSS and Surfactant. Polymer-Plastics Technology and Engineering, 2011, 50, 73-79.	1.9	10
71	Preparation and Characterizations of Novel PS Composites Containing OctaTMA-POSS-based Lamellar Hybrids. International Journal of Polymeric Materials and Polymeric Biomaterials, 2011, 60, 947-958.	1.8	8
72	Synthesis and characterization of AB block copolymers based on polyhedral oligomeric silsesquioxane. Journal of Polymer Research, 2010, 17, 19-23.	1.2	16

#	Article	IF	CITATIONS
73	Mesoporous hybrid from anionic polyhedral oligomeric silsesquioxanes (POSS) and cationic surfactant by hydrothermal approach. Microporous and Mesoporous Materials, 2010, 132, 567-571.	2.2	11
74	Lamellar hybrid from octa(γ-chloroaminopropyl) polyhedral oligomeric silsesquioxanes and anionic surfactant by ion-exchange reaction. Materials Letters, 2007, 61, 1077-1081.	1.3	13
75	Combustion and thermal properties of OctaTMA-POSS/PS composites. Journal of Materials Science, 2007, 42, 4325-4333.	1.7	59
76	Synthesis and characterization of ion-exchangeable layered Octabenzenesulphonate Polyhedral Oligomeric Silsesquioxanes modified by surfactant. Materials Letters, 2006, 60, 1823-1827.	1.3	10